Journal of Statistical Physics, Vol. 57, Nos. 3/4, 1989

Mode-Coupling Effects in the Density Dependence of the Shear Viscosities of Dense Argon and Methane

I. M. de Schepper,[1] J. J. van Loef,[1] and A. F. E. M. Haffmans[1]

Received February 24, 1989

We argue that the density dependence of the shear viscosities of dense argon at 174, 223, and 301 K and of dense methane at 298 K can be understood on the basis of the mode coupling theory for hard spheres, in particular near the fluid–solid phase transition.

KEY WORDS: Shear viscosity; mode coupling theory; Enskog theory; hard spheres; argon; methane.

1. INTRODUCTION

Recently it was shown that the large increase of the shear viscosity η of hard-sphere fluids near the fluid–solid transition[1,2] can be understood using the Enskog theory and, in addition, the mode coupling theory, which is complementary to the Enskog theory.[3–7] Here we show that the hard-sphere results are relevant also for the density dependence of η of argon at the temperatures $T = 174$, 223, and 301 K and methane at $T = 298$ K, using equivalent hard-sphere diameters for these fluids. In fact, the fluidities $\phi = 1/\eta$ of very dense argon and methane depend linearly on the volume V and vanish when V is near the solid volume, very similar to the behavior of ϕ of hard-sphere fluids, as predicted by kinetic theory.

We summarize the hard-sphere kinetic theory results in Section 2, and discuss the argon data in Section 3 and the methane data in Section 4. We end with a discussion in Section 5.

[1] IRI, University of Delft, 2629 JB Delft, The Netherlands.

0022-4715/89/1100-0631$06.00/0

822/57/3-4-14

2. HARD SPHERES

The shear viscosity of a monatomic fluid is, for any interparticle potential, given by the Green–Kubo time integral,[8,9]

$$\eta = \int_0^\infty dt\, \rho(t) \tag{1}$$

where $\rho(t)$ is the stress tensor autocorrelation function given by

$$\rho(t) = \frac{m^2 n}{k_B T} \langle J_{xy} e^{tL} J_{xy} \rangle \tag{2}$$

Here, k_B is Boltzmann's constant, m is the mass of the particles, $n = N/V$ is the number density, with N the number of particles and V the volume of the fluid, J_{xy} is the x, y component of the microscopic stress tensor, L is the Liouville operator, and the brackets denote the canonical equilibrium ensemble average at temperature T and density n. The streaming operator $\exp(tL)$ in Eq. (2) replaces all positions $\mathbf{r}_j$ and $\mathbf{v}_j$ of the particles $j = 1,..., N$ by those a time t later. For differentiable interparticle potentials, J_{xy} and L are given by Eqs. (A2) and (A12) of Appendix A, respectively.

Then, for hard spheres[3–7]

$$\rho(t) = \rho_E(t) + \rho_{mc}(t) \tag{3}$$

where $\rho_E(t)$ and $\rho_{mc}(t)$ are the contributions to $\rho(t)$ according to the Enskog and mode-coupling theories, respectively. The contribution $\rho_E(t)$ to $\rho(t)$ dominates $\rho(t)$ for *short* times[10] (i.e., $0 \leqslant t \leqslant 5t_E$), vanishes proportionally to $\exp(-t/t_E)$ for large times (i.e., $t \gg 5t_E$), and satisfies

$$\eta_E = \int_0^\infty dt\, \rho_E(t) \tag{4}$$

where η_E is the Enskog value of the shear viscosity.[11] Here t_E is the mean free time between collisions. An explicit expression for η_E is given in ref. 11.

The mode coupling contribution $\rho_{mc}(t)$ to $\rho(t)$ in Eq. (3) increases from 0 at $t = 0$ to a maximum value near $t = 5t_E$ and is given for *large* times, i.e., $t \geqslant 10t_E$, by[3]

$$\rho_{mc}(t) = \frac{m^2 n}{k_B T} \frac{1}{2} \frac{V}{(2\pi)^3} \sum_{i,j} \int d\mathbf{k}\, V_{ij}(\mathbf{k}) \exp\{-[z_i(k) + z_j(k)]\, t\} \tag{5}$$

where $\mathbf{k}$ is a wave vector with length $k = |\mathbf{k}|$ and where both i and j run over the five $\mathbf{k}$-dependent (Enskog) extended hydrodynamic modes of the

fluid, i.e., the extended heat mode i or $j=h$, the two extended sound modes i or $j=\pm$, and the two extended shear modes i or $j=\eta_{1,2}$.

The five extended hydrodynamic modes[12-14] are defined as those five eigenvalues $z_i(k)$ and corresponding eigenfunctions $\psi_i(\mathbf{k})$ of the inhomogeneous Enskog operator $L_E(\mathbf{k})$ which are the extensions of the hydrodynamic eigenmodes of $L_E(\mathbf{k})$ for $k \to 0$ to larger values of k.

We note here that the inhomogeneous Enskog operator $L_E(\mathbf{k})$ effectively replaces the Liouville operator L in the time evolution of microscopic $\mathbf{k}$-dependent single-particle correlation functions.[15] Explicit expressions for the vertex functions $V_{ij}(\mathbf{k})$ in Eq. (5) are given in ref. 3 in terms of the eigenfunctions $\psi_l(\mathbf{k})$ of $L_E(\mathbf{k})$ and of the static equilibrium correlation functions of the fluid. In fact, each $V_{ij}(\mathbf{k})$ arises from the coupling of the microscopic stress tensor J_{xy} to the product of the single-particle modes $\psi_i(\mathbf{k})$ and $\psi_j(-\mathbf{k})$.

To evaluate $\rho_{mc}(t)$, one distinguishes two regions in the $\mathbf{k}$ integral on the right-hand side of Eq. (5), i.e., small and large k values, respectively.

2.1. Small k

For small k the five eigenvalues $z_i(k)$ are given by[16] $z_h(k)=a_E k^2$ for the heat mode, $z_\pm(k)=\pm ick+\Gamma_E k^2$ for the two sound modes, and $z_{\eta_1}(k)=z_{\eta_2}(k)=\eta_E k^2/mn$ for the two shear modes. Here c is the speed of sound and a_E and Γ_E are the Enskog values of the thermal diffusivity and sound damping, respectively. The five corresponding eigenfunctions $\psi_j(\mathbf{k})$ are, in general, linear combinations of the five microscopic quantities: the density, the temperature, and the three components of the microscopic velocity. The heat mode eigenfunction $\psi_h(\mathbf{k})$ is, in particular, a linear combination of the microscopic density and microscopic temperature alone. These results are valid in the so-called hydrodynamic regime, i.e., for $0 \leqslant k\sigma < 1$, where σ is the diameter of the hard spheres.

Then, by performing the $\mathbf{k}$ integral on the right-hand side of Eq. (5) with $0 \leqslant k\sigma < 1$ one finds for $t \geqslant 10t_E$ that $\rho_{mc}(t)=\alpha t^{-3/2}$, which is the well-known long-time tail in $\rho(t)$, extensively studied during the past 15 years.[9,10,16,17] The coefficient α of the long-time tail $\sim t^{-3/2}$ in $\rho(t)$ involves both thermodynamic and (Enskog) transport properties of the fluid and is given explicitly, e.g., in ref. 17.

It has been found[7] that the time integral (with $t \geqslant 10t_E$) over this long-time tail yields contributions to the viscosity η [cf. Eqs. (1) and (3)] which amount to at most a few percent of η_E for all densities. Therefore, these so-called "conventional" mode coupling contributions to $\rho(t)$ are far too small to explain the behavior of η at high densities and will be neglected in the following.

2.2. Large k

For large k, i.e., $k\sigma > 1$, the two extended sound mode eigenvalues $z_{\pm}(k)$ and the two extended shear mode eigenvalues $z_{\eta_1}(k)$ and $z_{\eta_2}(k)$ are of the order of t_E^{-1} for all densities. Therefore, their contributions to $\rho_{mc}(t)$ in Eq. (5) are negligible for all densities, since $t \geqslant 10 t_E$. Also, the extended heat mode eigenvalue $z_h(k)$ is of the order of t_E^{-1} for all $k\sigma > 1$ and all reduced densities $n^* = n\sigma^3 < 0.7$. This implies that *all* contributions to $\rho_{mc}(t)$ in Eq. (5) are negligible when $n^* < 0.7$, so that η is in good approximation given by η_E for all $n^* < 0.7$. This result is consistent with the exact theoretical low-density expansion of η,[18] and with molecular dynamics (MD) data,[19] which also show that $\eta \approx \eta_E$ (within a few percent) when $n^* < 0.7$.

Thus, we restrict ourselves in the following to $n^* \geqslant 0.7$ and to the contributions of two extended heat modes to $\rho_{mc}(t)$ in Eq. (5).

On the basis of numerical calculations for $k\sigma > 1$ and $n^* \geqslant 0.7$ it has been shown[12-14] that $z_h(k)$ lies far below all other eigenvalues of $L_E(\mathbf{k})$. In addition, $z_h(k)$ shows a pronounced minimum $z_h(k^*)$ at $k = k^*$ with $k^*\sigma$ near 2π, which decreases linearly with increasing density, as

$$z_h(k^*) = 4.18(1.056 - n^*)\, t_\sigma^{-1} \tag{6}$$

where $t_\sigma = (m/4k_B T)^{1/2}\,\sigma$. To understand this result, one uses the fact[4,5,12] that there are two very different length scales in the fluid, i.e., the diameter σ and the mean free path between collisions l, with two corresponding time scales t_σ and t_E, respectively. Here, $t_\sigma/t_E = (2/\pi)^{1/2}\,\sigma/l = 2(\pi)^{1/2}\, g(\sigma)\, n^*$, with $g(\sigma)$ the pair correlation function $g(r)$ at contact. Thus, for increasing densities, l and t_E become increasingly smaller than σ and t_σ, respectively. Then, using l/σ (or t_E/t_σ) as a small expansion parameter in the Enskog theory, one finds to lowest nonvanishing order in l/σ that for $1 < k\sigma < \sigma/l$,[20]

$$z_h^{(0)}(k) = \frac{D_E k^2}{S(k)}\, d(k) \tag{7}$$

with a corresponding eigenvector $\psi_h^{(0)}(\mathbf{k})$ which is the microscopic density alone, and

$$V_{hh}^{(0)}(\mathbf{k}) = \frac{1}{N}\left[\frac{k_B T}{m}\frac{k_x k_y}{kS(k)}\frac{\partial S(k)}{\partial k}\right]^2 \tag{8}$$

where k_x and k_y are the x and y components of the wavevector $\mathbf{k}$, respectively. In Eq. (7), $S(k)$ is the static structure factor, D_E is the Enskog value

of the self-diffusion coefficient D, and $d(k)$ is a density-independent, dimensionless function of $k\sigma$ of order 1, given by

$$d(k)=\frac{1}{1-j_0(k\sigma)+2j_2(k\sigma)} \tag{9}$$

with $j_n(x)$ the spherical Bessel function of order n. The superscript zero in $z_h^{(0)}(k)$ and $V_{hh}^{(0)}(k)$ denotes that these quantities are equal to $z_h(k)$ and $V_{hh}(k)$, respectively, when l/σ is very small, i.e., for very high densities.

We note here that the extended heat mode, which is the heat mode for $k\sigma<1$, has changed its character for $k\sigma>1$ to a densitylike or, rather, a self-diffusion-like mode, since the component of the eigenvector $\psi_h(\mathbf{k})$ on the microscopic temperature has vanished then.

Now, in Eq. (7), the minimum in $z_h^{(0)}(k)$ at $k=k^*(n)$ is caused by the first maximum in $S(k)$ near $k=k^*(n)$, where $k^*(n)\simeq 2\pi/\sigma$ depends slightly on n, since the location of the maximum in $S(k)$ depends slightly on n. The minimum value $z_h^{(0)}(k^*)$ of $z_h(k)$ is therefore determined (1) by D_E, which strongly decreases, (2) by $S(k^*)$, which strongly increases, and (3) by k^{*2} and $d(k^*)$, which are virtually constant, when n increases. These dependences together lead to the linear behavior in n^* of $z_h(k^*)$ given by Eq. (6).[20] The contribution to $\rho_{mc}(t)$ in Eq. (5) of two extended heat modes $i=h$ and $j=h$ with $k\sigma>1$ has been called the "extended" mode coupling contribution to $\rho(t)$,[7] and will be considered here further.

One finds from Eqs. (5), (7), and (8) that for $n^*>0.7$ the extended mode coupling contribution $\rho_{mc}(t)$ to $\rho(t)$ arises mainly from the region $3\lesssim k\sigma\lesssim 8$ around $k^*\sigma\simeq 2\pi$, where $z_h(k)$ is minimal, so that $\rho_{mc}(t)\sim\exp[-2z_h(k^*)\,t]$ for $t\geqslant 10t_E$. It appears that this extended mode coupling tail $\sim\exp[-2z_h(k^*)\,t]$ in $\rho(t)$ is much larger than the conventional tail $\alpha t^{-3/2}$, e.g., for $n^*=0.884$ and $t\simeq 15t_E$ it is about 400 times $\alpha t^{-3/2}$. Also, the contribution of $\rho_{mc}(t)$ to η increases with increasing density, since $z_h(k^*)$ decreases [cf. Eq. (6)], so that the tail $\sim\exp[-2z_h(k^*)\,t]$ increases.

We discuss the results for η in terms of the fluidity $\phi=1/\eta$, or, rather, the reduced fluidity ϕ^*, defined by

$$\phi^*=\frac{1}{\eta}\frac{(mk_BT)^{1/2}}{\sigma^2} \tag{10}$$

In Fig. 1 we show the results for ϕ_E^* obtained from the Enskog theory alone and for ϕ^* obtained from the Enskog and mode coupling theories together [cf. Eqs. (1)–(10)] as functions of the reduced volume

$$V^*=n^{*-1}=V/N\sigma^3 \tag{11}$$

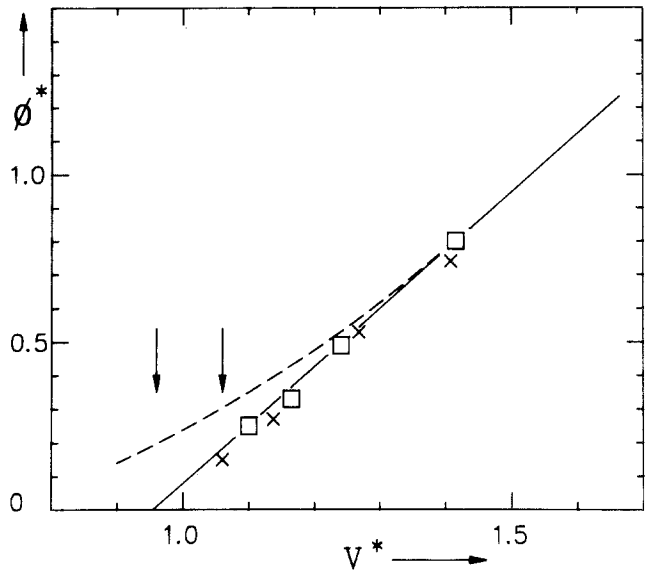

Fig. 1. Reduced hard-sphere fluidity ϕ^* [cf. Eq. (10)] as a function of the reduced volume V^* according to the Enskog theory (dashed curve), the mode coupling theory (solid curve), and MD simulations (squares from ref. 2 and crosses from ref. 1). The right arrow points to the reduced liquid volume at solidification $V_L^* = 1.06$ and the left arrow points to the reduced solid volume at melting $V_S^* = 0.961$. The solid and dashed curves are indistinguishable for $V^* > 1.4$.

One sees in Fig. 1 that $\phi^* = \phi_E^*$ for $V^* > 1.4$. This is due to the fact that the minimum $z_h(k^*)$ in $z_h(k)$ is not low enough to yield noticeable contributions to $\rho_{mc}(t)$ for $t \geqslant 10t_E$, so that $\eta = \eta_E$ then. Thus, the linear behavior $\phi^* = \phi_E^* = 1.7(V^* - 0.95)$ observed for $V^* > 1.4$ is due to the Enskog theory alone.

For $V^* < 1.4$, ϕ_E^* is not linear in V^* anymore and is finite down to the reduced liquid volume at solidification $V_L^* = 1.06$ and the reduced solid volume at melting $V_S^* = 0.961$.[21] However, when the mode coupling contribution is included, ϕ^* stays linear in V^*, i.e.,

$$\phi^* = 1.7(V^* - 0.95) \tag{12}$$

down to V_L^* and V_S^* (cf. Fig. 1). Therefore, ϕ^* (virtually) vanishes when V^* approaches V_S^* and η diverges then. This behavior is due to the vanishing of $z_h(k^*)$ when $n^* \to 1.056$ (or, equivalently, $V^* \to 0.95$) [cf. Eq. (6)], since then the tail $\sim \exp[-2z_h(k^*)\, t]$ in $\rho_{mc}(t)$ can no longer be integrated over t, so that $\eta \to \infty$. One sees in Fig. 1 that ϕ^* obtained from hard-sphere MD simulations[1,2] agrees well with the theoretical mode coupling prediction

for ϕ^*. Thus, we conclude that for hard spheres the apparent divergence of η (or vanishing of ϕ) can be understood on the basis of the (extended) mode coupling theory.

3. ARGON

We have two reasons to believe that the hard-sphere mode coupling result for ϕ^* [cf. Eq. (12) and Fig. 1] is relevant also for the reduced fluidity ϕ^* of dense argon.

First, the expression for the strength $V_{hh}^{(0)}(k)$ of the coupling of the microscopic stress tensor J_{xy} to two coupled microscopic normalized density modes, as given by Eq. (8) for hard spheres, is valid also for systems of particles interacting through a differentiable interparticle potential, such as argon. This has been noted by Kirkpatrick.[4,22] The proof[22] is explicitly given in the Appendix.

Second, according to the Enskog theory, the half-width at half-height $\omega_H(k)$ of the dynamic structure factor $S(k, \omega)$, observed in neutron scattering experiments, is almost completely given by $z_h(k)$ when $k\sigma > 1$, i.e., then $\omega_H(k) = z_h(k)$.[13] Indeed, the experimentally observed values for $\omega_H(k)$ obtained from neutron scattering experiments on $S(k, \omega)$ for liquid argon at $T = 120$ K and four (high) densities[23] are in very good agreement with the hard-sphere $z_h(k)$ given by Eqs. (6) and (7) when $\sigma = 3.44$ Å for the argon atoms at $T = 120$ K.[13,20]

Thus, the two basic quantities $V_{hh}^{(0)}(k)$ and $z_h^{(0)}(k)$ in the (extended) mode coupling theory for hard spheres appear to be relevant also for argon, at least for $T = 120$ K with $\sigma = 3.44$ Å. We note that the equivalent hard-sphere diameter $\sigma = 3.44$ Å for argon at 120 K has been obtained in three independent ways.[13,20] First, we determined $\sigma^{(Sk)}$ as that value of σ for which the static structure factor $S(k)$ of (dense) argon around the first maximum near $k\sigma = 2\pi$[23] fits best to the $S(k)$ of a hard-sphere fluid. Second and third, we determined $\sigma^{(L)}$ and $\sigma^{(S)}$ as those values of σ for which the liquid volume (per particle) at solidification V_L and the solid volume (per particle) at melting V_S, respectively, coincide for argon and hard spheres, so that

$$\sigma^{(L)} = (V_L/1.06)^{1/3} \tag{13}$$

and

$$\sigma^{(S)} = (V_S/0.961)^{1/3} \tag{14}$$

where the V_L and V_S of argon are given in Table I (cf. refs. 24–26) as functions of T. Thus, one finds for argon at 120 K that

Table I. Liquid Volume per Particle at Solidification V_L, Solid Volume per Particle at Melting V_S, Equivalent Hard-Sphere Diameters $\sigma^{(i)}$ Obtained from $V_L(i=L)$, $V_S(i=S)$, and $S(k)$ $(i=Sk)$, and Lennard-Jones Parameters for Argon and Methane[a]

	Ar	Ar	Ar	Ar	CH_4
T, K	120	174	223	301	298
V_L, Å^3	43.1	39.5	37.2	34.7	43 ± 1
V_S, Å^3	39.2	36.9	35.2	33.2	—
$\sigma^{(L)}$, Å	3.44	3.34	3.27	3.19	3.44 ± 0.03
$\sigma^{(S)}$, Å	3.45	3.37	3.32	3.26	—
$\sigma^{(Sk)}$, Å	3.43	3.37[a]	3.33[a]	3.27[a]	3.64[a]
ε_{LJ}/k_B, K	123.2	123.2	123.2	123.2	156.1
σ_{LJ}, Å	3.36	3.36	3.36	3.36	3.70

[a] Values obtained from the mean spherical approximation for $S(k)$ of the corresponding Lennard-Jones fluids.

$\sigma^{(Sk)} \simeq \sigma^{(S)} \simeq \sigma^{(L)} = 3.44$ Å (cf. Table I), so that the three methods to obtain σ are similar at 120 K. However, we find that the three methods became gradually less similar when T increases, since then $\sigma^{(L)}$ becomes increasingly smaller than $\sigma^{(Sk)} \simeq \sigma^{(S)}$, which are still very close (cf. Table I).

We remark that, in fact, $\sigma^{(Sk)}$ in Table I is determined using the mean spherical approximation for $S(k)$,[27] assuming that argon is a Lennard-Jones fluid with the Lennard-Jones parameters σ_{LJ} and ε_{LJ}/k_B given in Table I. However, one finds that this theoretical $S(k)$ is in perfect agreement with the experimental neutron scattering data for $S(k)$ at $T = 120$ K.[23]

Now, we consider the experimental argon data for ϕ^* at $T = 174$, 223, and 301 K[28–31] using $\sigma^{(L)} = \sigma$ as the equivalent hard-sphere diameter σ in Eqs. (10) and (11) (cf. Table I). We show the results for ϕ^* as a functions of V^* in Fig. 2. Observe that the argon data for ϕ^* agree increasingly well with the hard-sphere mode coupling theory result for ϕ^* [the straight line given by Eq. (12)] when the density increases, i.e., when V^* decreases. In particular, the agreement is very good at all three temperatures when $V^* < 1.35$ (cf. Fig. 2). We note that for $V^* < 1.35$, the agreement between the experimental ϕ^* and theoretical ϕ^* becomes increasingly less when T increases if one uses $\sigma^{(Sk)} \simeq \sigma^{(S)}$ as the equivalent hard-sphere diameter of the argon atoms. Thus, the density dependence of the fluidity ϕ of argon at three temperatures can be understood on the basis of the mode coupling theory for hard spheres, in particular, if one uses $\sigma^{(L)}$ as the equivalent hard-sphere diameter of the argon atoms.

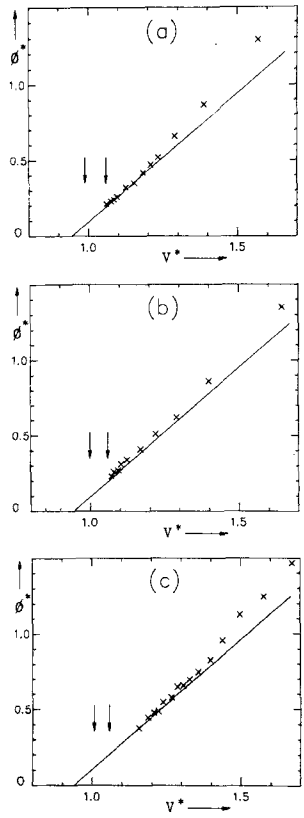

Fig. 2. Reduced argon fluidity ϕ^* [cf. Eq. (10)] (crosses) as a function of the reduced volume V^* at (a) $T = 174$ K, $\sigma = 3.34$ Å; (b) $T = 223$ K, $\sigma = 3.27$ Å; and (c) $T = 301$ K, $\sigma = 3.19$ Å. The solid curve is ϕ^* from hard-sphere mode-coupling theory (cf. Fig. 1). The right and left arrows point to V_L^* and V_S^* of argon, respectively.

4. METHANE

In order to see whether the hard-sphere mode coupling theory is relevant also for systems more complicated than a noble gas fluid like argon, we consider the recent results for $\phi = 1/\eta$ obtained for methane at 298 K.[32]

In Fig. 3 we show the reduced methane fluidity ϕ^* as function of V^* [cf. Eqs. (10) and (11)] with $\sigma = 3.54$ Å. Here $\sigma = 3.54$ Å is the equivalent hard-sphere diameter of methane for which the experimental ϕ^* fit best to the theoretical prediction for ϕ^* given by Eq. (12). Observe in Fig. 3 that the agreement between theory and experiment is very good up to about $V^* = 1.5$.

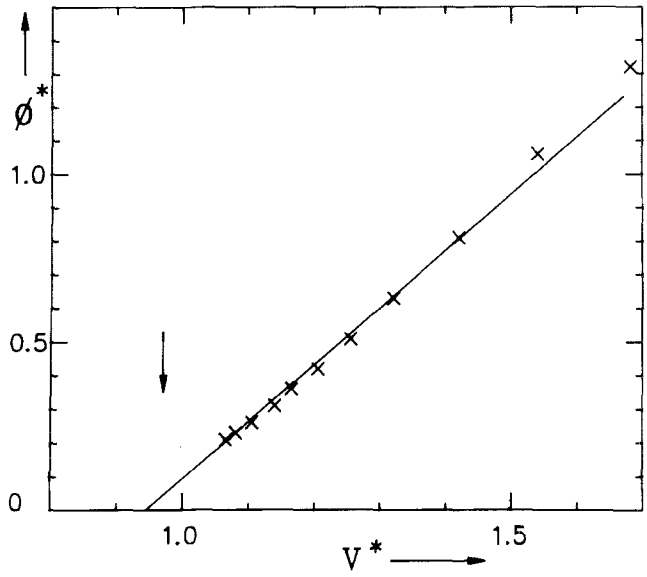

Fig. 3. Reduced methane fluidity ϕ^* [cf. Eq. (10)] (crosses) as a function of the reduced volume V^* at $T = 298$ K with $\sigma = 3.54$ Å. The solid curve is ϕ^* from hard-sphere mode-coupling theory (cf. Fig. 1). The arrow points to V_L^* of methane.

We remark that the value $\sigma = 3.54$ Å differs significantly from both $\sigma^{(L)}$ (ref. 33) and $\sigma^{(Sk)}$ for methane at this temperature (cf. Table I). Since we could not find reliable data for V_S of methane at 298 K, a comparison of $\sigma = 3.54$ Å with $\sigma^{(S)}$ of methane [cf. Eq. (14)] cannot be made here. We conclude from Fig. 3 and Table I that the fluidity of methane at 298 K is very hard-sphere-like, albeit that an identification of the equivalent hard-sphere diameter for methane needed in the numerical comparison is still lacking.

5. DISCUSSION

Using an appropriately chosen equivalent hard-sphere diameter σ, we find that the reduced fluidity $\phi^*(V^*)$ of argon at 174, 223, and 301 K and methane at 298 K [cf. Eqs. (10) and (11)] shows, for reduced volume $V^* < 1.3$, a linear behavior in V^* which agrees very well with the hard-sphere (extended) mode coupling theory prediction for $\phi^*(V^*)$ given by Eq. (12) (cf. Figs. 2 and 3). From this good agreement we conclude that the vanishing of ϕ near the fluid–solid phase transition observed in real fluids like argon and methane might well be caused by the same basic physical mechanisms which cause the vanishing of ϕ in a hard-sphere fluid

(cf. Fig. 1). In particular, we expect for monatomic fluids in general the presence of an "extended heat mode" which should be, in fact, a self-diffusion-like mode with an inverse decay time $z_h(k)$ well represented by Eq. (7) for all $k\sigma > 1$ and by Eq. (6) for its minimum value $z_h(k^*)$. Thus, the viscosity η will diverge and the fluidity ϕ will vanish for monatomic fluids in general in a similar fashion as for hard spheres, due to the peculiar behavior of $z_h(k)$ near $k = k^*$.

We end with a few remarks and open questions.

(a) From the good agreement in Fig. 2 it follows that $\sigma^{(L)}$ [cf. Eq. (13)] is the equivalent hard-sphere diameter of argon most relevant for the comparison of the fluidities of argon and hard spheres. Why $\sigma^{(L)}$ is more relevant than, e.g., $\sigma^{(S)}$ or $\sigma^{(Sk)}$ (cf. Table I) is unclear at present. However, one might expect that neutron scattering experiments on argon for $T > 120$ K will yield results for the half-widths $\omega_H(k)$ of $S(k, \omega)$ which agree better with the hard-sphere $z_h(k)$ [cf. Eqs. (6) and (7)] when one uses $\sigma^{(L)}$ rather than $\sigma^{(S)} \simeq \sigma^{(Sk)}$ as the equivalent hard-sphere diameter of argon. This is presently under investigation.

(b) One sees in Fig. 2 that the reduced fluidity $\phi^*(V^*)$ of argon is virtually independent of the temperature. This implies [cf. Eq. (10)] that, apart from a hard-sphere factor $T^{-1/2}$, the temperature dependence of the absolute fluidity $\phi(V, T)$ or argon is determined by the temperature dependence of $\sigma = \sigma^{(L)}$, or, equivalently, by that of V_L [cf. Eq. (13)]. To understand this result, one needs to investigate the special role of $\sigma^{(L)}$ (or V_L) for the fluidity of argon at high densities.

(c) A more extended comparison of the fluidities of the light hydrocarbons CH_4, C_2H_4, C_2H_6, and C_3H_8 with those of a hard-sphere fluid might well reveal the special role of the equivalent hard-sphere diameter $\sigma = 3.54$ Å found here for CH_4 at 298 K (cf. Fig. 3).

(d) The (extended) mode coupling theory, when applied to the thermal conductivity λ in a manner completely similar to that discussed in this paper for η, leads to a vanishing mode coupling contribution to λ at high densities, for the microscopic heat current is odd in the microscopic velocities and therefore does not couple to two microscopic density modes (cf. Appendix). This result is consistent with the experimentally observed values of λ, which do not show any divergence near the fluid–solid transition.[31,34] The (extended) mode coupling theory applied to the self-diffusion coefficient D and the bulk viscosity ζ predicts that D vanishes[12] and that ζ diverges at very high densities. A comparison of these results with the (scarce) experimental data for D and ζ has not been made yet.

APPENDIX

Here we derive Eq. (8) for $V_{hh}^{(0)}$ for a monatomic fluid of N particles interacting through an arbitrary, but differentiable, interparticle potential $\phi(\mathbf{r})$, which is spherically symmetric.

The strength of the coupling of the microscopic stress tensor J_{xy} to the normalized microscopic density modes $\psi_h(\mathbf{k})$ is given by[4]

$$V_{hh}^{(0)}(k) = \{\langle J_{xy}\psi_h(\mathbf{k})\,\psi_h(-\mathbf{k})\rangle\}^2 \tag{A1}$$

where

$$J_{xy} = \frac{1}{\sqrt{N}} \sum_{j=1}^{N} \left[v_{j,x} v_{j,y} - \frac{1}{2m} \sum_{\substack{l=1 \\ l\neq j}}^{N} \frac{\partial\phi(\mathbf{r}_{jl})}{\partial x_{jl}}\, y_{jl} \right] \tag{A2}$$

and

$$\psi_h(\mathbf{k}) = \frac{1}{\sqrt{S(k)}}\, n(\mathbf{k}) \tag{A3}$$

Here $v_{j,x}$ and $v_{j,y}$ are the x and y components of $\mathbf{v}_j$, respectively, x_{jl} and y_{jl} are the x and y components of $\mathbf{r}_{jl} = \mathbf{r}_j - \mathbf{r}_l$, respectively, $n(\mathbf{k})$ is the (unnormalized) microscopic density given by

$$n(\mathbf{k}) = \frac{1}{\sqrt{N}} \sum_{j=1}^{N} \exp(-i\mathbf{k}\cdot\mathbf{r}_j) \tag{A4}$$

and $S(k)$ is the static structure factor, given by

$$S(k) = \langle n(\mathbf{k})^*\, n(\mathbf{k})\rangle \tag{A5}$$

so that $\psi_h(\mathbf{k})$ is normalized to 1 for all k, i.e.,

$$\langle \psi_h(\mathbf{k})^*\, \psi_h(\mathbf{k})\rangle = 1 \tag{A6}$$

Thus, from Eqs. (A1) and (A3) one obtains

$$V_{hh}^{(0)}(k) = \left[\frac{1}{S(k)} \langle J_{xy} n(\mathbf{k})\, n(-\mathbf{k})\rangle \right]^2 \tag{A7}$$

Next we use that J_{xy} is the $q=0$ limit of the wavevector ($\mathbf{q}$)-dependent microscopic stress tensor $\tau_{xy}(\mathbf{q})$, i.e.,

$$J_{xy} = \lim_{q\to 0} \tau_{xy}(\mathbf{q}) \tag{A8}$$

where $\mathbf{q}$ is in the y direction and

$$\tau_{xy}(\mathbf{q}) = \frac{1}{\sqrt{N}} \sum_{j=1}^{N} \left\{ v_{j,x} v_{j,y} + \frac{i}{2mq} \sum_{\substack{l=1 \\ l \neq j}}^{N} \frac{\partial \phi(\mathbf{r}_{jl})}{\partial x_{jl}} \times [\exp(i\mathbf{q} \cdot \mathbf{r}_{jl}) - 1] \right\} \exp(-i\mathbf{q} \cdot \mathbf{r}_j) \tag{A9}$$

with $q = |\mathbf{q}|$. Thus,

$$V_{hh}^{(0)}(k) = \frac{1}{S(k)^2} \lim_{q \to 0} [\langle \tau_{xy}(\mathbf{q})\, n(\mathbf{k})\, n(-\mathbf{k}-\mathbf{q}) \rangle]^2 \tag{A10}$$

where we have replaced $n(-\mathbf{k})$ in Eq. (A7) by $n(-\mathbf{k}-\mathbf{q})$ in Eq. (A10) to obey momentum conservation, i.e., the sum of the wavevectors in the average on the right-hand side of Eq. (A10) must vanish. Then we use that

$$Lu_x(\mathbf{q}) = -iq\tau_{xy}(\mathbf{q}) \tag{A11}$$

where L is the Louville operator of the fluid, i.e.,

$$L = \sum_{j=1}^{N} \left[\mathbf{v}_j \cdot \frac{\partial}{\partial \mathbf{r}_j} - \frac{1}{m} \sum_{\substack{l=1 \\ l \neq j}}^{N} \frac{\partial \phi(\mathbf{r}_{jk})}{\partial \mathbf{r}_{jl}} \cdot \frac{\partial}{\partial \mathbf{v}_l} \right] \tag{A12}$$

and $u_x(\mathbf{q})$ is the x component of the microscopic velocity $\mathbf{u}(\mathbf{q})$ given by

$$\mathbf{u}(\mathbf{q}) = \frac{1}{\sqrt{N}} \sum_{j=1}^{N} \mathbf{v}_j \exp(-i\mathbf{q} \cdot \mathbf{r}_j) \tag{A13}$$

Therefore [cf. Eqs. (A10) and (A11)]

$$V_{hh}^{(0)}(k) = \frac{-1}{S(k)^2} \lim_{q \to 0} \frac{1}{q^2} \{ \langle [Lu_x(\mathbf{q})]\, n(\mathbf{k})\, n(-\mathbf{k}-\mathbf{q})) \rangle \}^2 \tag{A14}$$

Then, using that L is an anti-Hermitian differential operator, one has

$$V_{hh}^{(0)}(k) = \frac{-1}{S(k)^2} \lim_{q \to 0} \frac{1}{q^2} [\langle u_x(\mathbf{q})\, n(-\mathbf{k}-\mathbf{q})\, Ln(\mathbf{k}) \rangle + \langle u_x(\mathbf{q})\, n(\mathbf{k})\, Ln(-\mathbf{k}-\mathbf{q}) \rangle]^2 \tag{A15}$$

Finally [cf. Eqs. (A4), (A5), (A12), and (A13)]

$$Ln(\mathbf{k}') = -i\mathbf{k}' \cdot \mathbf{u}(\mathbf{k}') \tag{A16}$$

and

$$\langle u_\alpha(\mathbf{q}')\, u_\beta(\mathbf{k}')\, n(-\mathbf{k}'-\mathbf{q}')\rangle = \frac{1}{\sqrt{N}} \frac{k_B T}{m} \delta_{\alpha\beta} S(|\mathbf{k}'-\mathbf{q}'|) \tag{A17}$$

for any two wavevectors $\mathbf{k}'$ and $\mathbf{q}'$. Thus, with $\mathbf{q}$ in the y direction,

$$V_{hh}^{(0)}(k) = \frac{1}{N}\left(\frac{k_B T k_x}{mS(k)}\right)^2 \lim_{q\to 0} \frac{1}{q^2} [S(|\mathbf{k}-\mathbf{q}|) - S(k)]^2 \tag{A18}$$

so that

$$V_{hh}^{(0)}(k) = \frac{1}{N}\left[\frac{k_B T}{m} \frac{k_x k_y}{kS(k)} \frac{\partial S(k)}{\partial k}\right]^2 \tag{A19}$$

which is the final result, used in Eq. (8) of the text.

ACKNOWLEDGMENT

This paper, dedicated to Prof. E. G. D. Cohen on the occasion of his 65th birthday, has profited very much from his vivid interest. Stimulating discussions with him are gratefully acknowledged.

REFERENCES

1. B. J. Alder, D. M. Gass, and T. E. Wainwright, *J. Chem. Phys.* **53**:3813 (1970).
2. J. P. J. Michels and N. J. Trappeniers, *Physica* **104A**:243 (1980).
3. H. van Beijeren, *Phys. Lett.* **105A**:191 (1984).
4. T. R. Kirkpatrick, *Phys. Rev. Lett.* **53**:1735, 2185 (1984).
5. T. R. Kirkpatrick and J. C. Nieuwoudt, *Phys. Rev. A* **33**:2651 (1986).
6. I. M. de Schepper, A. F. E. M. Haffmans, and H. van Beijeren, *Phys. Rev. Lett.* **56**:538 (1986).
7. I. M. de Schepper, A. F. E. M. Haffmans, and H. van Beijeren, *Phys. Rev. Lett.* **57**:1715 (1986).
8. J.-P. Hansen and I. R. McDonald, *Theory of Simple Liquids* (Academic, New York, 1976).
9. J. P. Boon and S. Yip, *Molecular Hydrodynamics* (McGraw-Hill, New York, 1980).
10. J. J. Erpenbeck and W. W. Wood, *J. Stat. Phys.* **24**:455 (1981).
11. S. Chapman and T. G. Cowling, *The Mathematical Theory of Nonuniform Gases* (Cambridge University Press, Cambridge, 1970).
12. I. M. de Schepper and E. G. D. Cohen, *Phys. Lett.* **68A**:308 (1978); *J. Stat. Phys.* **27**:223 (1982).
13. E. G. D. Cohen, I. M. de Schepper, and M. J. Zuilhof, *Physica* **127B**:282 (1984); *Phys. Lett.* **101A**:399 (1984).
14. B. Kamgar-Parsi, E. G. D. Cohen, and I. M. de Schepper, *Phys. Rev. A* **35**:4781 (1987).
15. E. G. D. Cohen and I. M. de Schepper, *J. Stat. Phys.* **46**:949 (1987).
16. J. R. Dorfman and E. G. D. Cohen, *Phys. Rev. A* **6**:776 (1972); **12**:292 (1975).

17. M. H. Ernst, E. H. Hauge, and J. M. J. van Leeuwen, *Phys. Rev. A* **4**:233 (1971); *J. Stat. Phys.* **15**:7 (1976).
18. B. Kamgar-Parsi and J. V. Sengers, *Phys. Rev. Lett.* **51**:2163 (1983).
19. W. E. Alley and B. J. Alder, *Phys. Rev. A* **27**:3158 (1983).
20. E. G. D. Cohen, P. Westerhuijs, and I. M. de Schepper, *Phys. Rev. Lett.* **59**:2872 (1987).
21. W. W. Wood, in *Fundamental Problems in Statistical Mechanics III*, E. G. D. Cohen, ed. (North-Holland, Amsterdam, 1975).
22. T. R. Kirkpatrick, private communication.
23. A. A. van Well, P. Verkerk, L. A. de Graaf, J. B. Suck, and J. R. D. Copley, *Phys. Rev. A* **31**:3391 (1985).
24. R. K. Crawford and W. B. Daniels, *Phys. Rev. Lett.* **21**:367 (1968).
25. S. M. Stishov and V. J. Fedosimov, *JETP Lett.* **14**:217 (1971).
26. V. M. Cheng, W. B. Daniels, and R. K. Crawford, *Phys. Lett.* **43A**:109 (1973).
27. W. G. Madden and S. A. Rice, *J. Chem. Phys.* **72**:4208 (1980).
28. N. J. Trappeniers, P. S. van der Gulik, and H. van den Hooff, *Chem. Phys. Lett.* **70**:438 (1980).
29. J. J. van Loef, *Physica* **124B**:305 (1984).
30. P. S. van der Gulik and N. J. Trappeniers, *Physica* **135A**:1 (1986).
31. J. J. van Loef and E. G. D. Cohen, *Physica* **156A**:522 (1989).
32. P. S. van der Gulik, R. Mostert, and H. van den Berg, *Physica* **151A**:153 (1988).
33. S. Angus, B. Armstrong, and K. M. de Reuck, *International Thermodynamic Tables of the Fluid State—5, Methane* (Pergamon, London, 1978).
34. J. J. van Loef, *Int. J. Thermophys.* **7**:125 (1986).